Journal Pre-proof

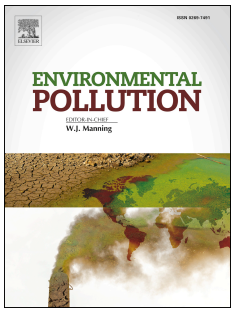

Remediation by waste marble powder and lime of jarosite-rich sediments from Portman Bay (Spain)

David Benavente, Concepcion Pla, Javier Valdes-Abellan, Silvia Cremades-Alted

PII: S0269-7491(19)37572-4

DOI: https://doi.org/10.1016/j.envpol.2020.114786

Reference: ENPO 114786

To appear in: *Environmental Pollution*

Received Date: 16 December 2019

Revised Date: 5 May 2020

Accepted Date: 8 May 2020

Please cite this article as: Benavente, D., Pla, C., Valdes-Abellan, J., Cremades-Alted, S., Remediation by waste marble powder and lime of jarosite-rich sediments from Portman Bay (Spain), *Environmental Pollution* (2020), doi: https://doi.org/10.1016/j.envpol.2020.114786.

Jarosite-rich sediments contaminated with heavy metals

$(K,H_3O)Fe_3(SO_4)_2(OH)_6$

[Mn, Cu, Zn, Cd, Cr, Ni, As]

Remediation treatments

Commercial hydrated limes

Waste marble powders

Mineralogical and geochemical characterisation

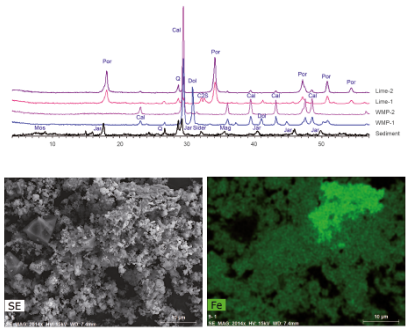

Geochemical modelling

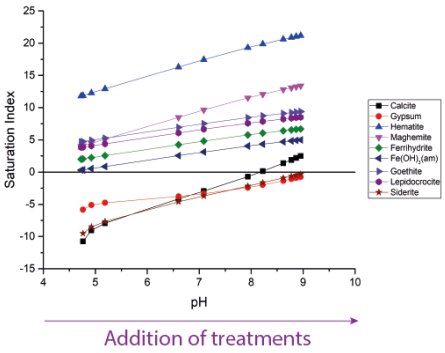

Addition of treatments

Remediation by waste marble powder and lime of jarosite-rich sediments from Portman Bay (Spain)

David Benavente[a], Concepcion Pla[b], Javier Valdes-Abellan[b], Silvia Cremades-Alted[a]

[a] Department of Earth and Environmental Sciences, University of Alicante (Spain)

[b] Department of Civil Engineering, University of Alicante (Spain)

** Corresponding author:*

D. Benavente

Department of Earth and Environmental Sciences, University of Alicante, Carretera San Vicente del Raspeig s/n, 03690 San Vicente del Raspeig (Alicante), Spain

david.benavente@ua.es

Tef./FAX: +0034 96590 3737

Email list:

D. Benavente: david.benavente@ua.es

C. Pla: c.pla@ua.es

J. Valdes-Abellan: javier.valdes@ua.es

S. Cremades-Alted: silvia140996@gmail.com

ORCID list:

D. Benavente: 0000-0001-7325-4042

C. Pla: 0000-0002-4269-2426

J. Valdes-Abellan: 0000-0003-3570-4983

Abstract

We investigate the use of hydrated lime and calcite waste marble powder as remediation treatments of contaminated jarosite-rich sediments from Portman Bay (SE, Spain), one of the most contaminated points in the Mediterranean coast by mining-metallurgical activities. We tested two commercial hydrated limes with different $Ca(OH)_2$ percentages (28 and 60 % for Lime-1 and Lime-2 respectively) and two different waste marble powder, WMP, from the marble industry (60 and 96% of calcite for WMP-1 and WMP-2 respectively). Mixture and column experiments and modelling of geochemical reactions using PHREEQC were performed. Lime caused the precipitation of hematite, gypsum and calcite, whereas WMP treatments formed iron carbonates and hematite. The fraction of amorphous phases was mainly composed of iron oxides, hydroxides and oxyhydroxides that was notably higher in the lime treatment in comparison to the WMP treatment. The reactive surface area showed a positive trend with the amorphous phase concentration. Results highlighted the effectiveness of lime treatments, where Lime-2 showed a complete elimination of jarosite. Column experiments revealed a clear reduction of heavy metal concentration in the lixiviate for the treated sediments compared to the original sediments. Particularly, Lime-2 showed the highest reduction in the peak concentration of Fe, Mn, Zn and Cd. The studied treatments limited the stabilisation of Cr and Ni, whereas contrarily As increases in the treated sediment. PHREEQC calculations showed that the most concentrated heavy metals (Zn and Mn) are stabilized mainly by precipitation whereas Cu, Pb and Cd by a combination of precipitation and sorption processes. This chemical environment leads to the precipitation of stable iron phases, which sorb and co-precipitate considerable amounts of potentially toxic elements. Lime is significantly more effective than WMP, although it is recommended that the pH value of the mixture should remain below 9 due to the amphoteric behaviour of heavy metals.

Keywords

Metal Precipitation; Heavy Metals; Amorphous Phases; Solid Bases; Jarosite.

1. Introduction

Portman Bay (SE, Spain) is one of the most contaminated points in the Mediterranean coast by mining-metallurgical activities and conforms a relevant example of jarosite-rich contaminated site. Portman Bay has been widely studied in different topics related to mobility of potentially toxic elements and their influence on ecotoxicological and human health (Alorda-Kleinglass et al., 2019; Ben Hamed et al., 2017; Cesar et al., 2009; Conesa and Schulin, 2010; García-Lorenzo et al., 2014; Martínez-Sánchez et al., 2008; Orozco et al., 1993; Pérez-Sirvent et al., 2018; Pérez-Sirvent et al., 2011; Pérez-Sirvent et al., 2007; Pérez-Sirvent et al., 2016; Perez-Sirvent et al., 2014) as well as a potential beach placer iron deposit (Manteca et al., 2014). Portman Bay area was mined from the time of the Roman Empire to 1991 when the activity ceased. During most of its working life, the waste materials were discharged directly into the sea, originally in the inner part of the bay, but later on, the wastes were discharged farther offshore (García-Lorenzo et al., 2014; Martínez-Sánchez et al., 2008). The intensive mining activity discharged more than 57 million tonnes of waste materials which caused the filling up of the bay (Martínez-Sánchez et al., 2008). In 2015, the Spanish ministry and local governments started a restoration project where 2 Mm^3 of tailings are planned to be removed (Alorda-Kleinglass et al., 2019) (Fig. S1 of Supplementary Materials section displays the filling up area of the bay). As a consequence of this extended activity, waste materials have a complex spatial distribution along the bay, with graded bedding in some areas. The mineralogical composition of the landfills includes sulphides (galena, pyrite, and sphalerite), phyllosilicates (chlorite and muscovite), siderite, iron oxides, and alteration products such as jarosite, oxohydroxides, hexahydrite group minerals and copiapite. Besides, chemical residues from reagents (xanthates, cyanures) used in ore floatation, were also discharged with the mining wastes (Martínez-Sánchez et al., 2008).

Among those minerals, Jarosite $(K,H_3O)Fe_3(SO_4)_2(OH)_6$ is one of the most abundant in Portman Bay. Jarosite is a member of the isostructural jarosite-alunite group of minerals that occurs commonly in acidic (pH < 3) and oxic environments, which include sulphide ore deposits, fluvial environments contaminated by acid rocks or acid mine drainages, wastes from the metallurgical extractive industry, acid sulphate soils and clay seams and beds (Dutrizac and Jambor, 2000; Hudson-Edwards et al., 1999; Smith et al., 2006).

Jarosite is of considerable geological, environmental, and metallurgical interest because it incorporates in its structure, sorbs and co-precipitates considerable amounts of potentially toxic elements such as As, Cr, Cd and Pb (Domènech et al., 2002; Dutrizac et al., 1980;

Dutrizac et al., 1996; Dutrizac et al., 1987; González-Ibarra et al., 2016; Gunneriusson et al., 2009; Smith et al., 2006). Specifically, several studies focused on the decomposition process of jarosite-type compounds in alkaline conditions have shown the metallurgical interest for the recovery of the contained metallic values (As, Zn, Cr, among others) (Mireles et al., 2016; Patiño et al., 2003; Patiño et al., 1998; Roca et al., 2006; Roca et al., 1993; Salinas et al., 2001).

Jarosite is relatively soluble and consequently, heavy metals incorporated in its structure can easily leak to the surrounding waters, which would turn into a major environmental problem affecting the aquatic related systems (Durães et al., 2017; Tang et al., 2018). These heavy metals may adversely affect soil ecology, agricultural production and water quality (Wang et al., 2001). Dissolved metals in waters may be stabilised when removed from acid conditions to alkaline environments (pH>7) by presumably converting them into oxide or oxyhydroxide phases. Most metals oxides or oxyhydroxides exhibit amphoteric behaviour. In other words, they are less soluble around pH 6 to 9 and they become more soluble at lower and higher pH's (Langmuir, 1997). The main alteration product of the jarosite is goethite when the alteration occurs in alkaline environments (Gasharova et al., 2005; Qian et al., 2019; Stoffregen, 1993; Stoffregen et al., 2000), although other phases are also expected such as oxides (hematite and magnetite), hydroxides (ferrihydrite and amorphous $Fe(OH)_3$) or oxyhydroxide (lepidocrocite and amorphous FeOOH). However, very few studies are related to the behaviour and stability of toxic species in the structure of these compounds under alkaline environments (Patiño et al., 2013).

In situ chemical immobilisation is a remediation technique that decreases the concentration of dissolved contaminants by sorption on the solid phase and/or precipitation. A number of natural or synthetic materials, such as carbonates, phosphate rocks, cement, zeolites, municipal biosolids, and red mud have been recently tested in order to evaluate their ability to immobilise toxic trace metals (Patiño et al., 2013). Among them, mostly calcite ($CaCO_3$) and hydrated lime ($Ca(OH)_2$) have been widely used for environmental studies, fundamentally in acid mine drainage waters (Acero et al., 2007; Bangira et al., 2017; Macías et al., 2012; Rose and Elliott, 2000; Simón et al., 2005; Soler et al., 2008). The neutralising reactions of acidic waters are fast and efficient and increase pH values up to 7. Hydrated lime is some orders of magnitude more soluble compared to $CaCO_3$, resulting final pH values higher than 11 when lime is dissolved (Bangira et al., 2017). However, calcite is less costly and abundant either as geologic material or as industrial by-product. In particular, waste marble powder, WMP, is an

industrial by-product resulting from mining, sawing, shaping and polishing of commercial marbles. WMP disposals constitute one of the most important concerns of the stone industries, consequently using WMP in soil remediation also offers a sustainable solution to the environmental problems of the natural stone industrial waste deposition.

Perez-Sirvent et al., (2007 and 2011) investigated the chemical immobilisation of contaminated sediments of the Portman Bay by adding WMP generated in a nearby natural stone industry, which was composed of dolomite (60%), calcite (38%), quartz (1%) and feldspar (1%). Results concluded that the stabilisation and immobilisation of the heavy metals using the dolomite WMP was effective for the studied sediments. Although these results were promising, the use of this dolomite WMP could be enhanced using a more calcite WMP, which is common in the most of the commercial marble industry, as well as using lime, a worldwide construction material and even more reactive than calcite. Moreover, most investigations in jarosite-rich sediments focus on water remediation or industrial recovery, and, however, very few studies are related to mineral reaction in the treated sediment in terms of the behaviour and stability of toxic species within the formed minerals.

In this paper, we evaluated and compare the use of calcite waste marble powder and hydrated lime as remediation treatment of contaminated sediments by heavy metals in jarosite-rich sediments from Portman Bay. We also investigated the geochemical reactions between the jarosite rich-sediments and added solid bases. Particularly, we characterised the precipitation of iron phases and geochemically simulated the precipitation and sorption processes, with an emphasis on the amorphous phases and its role in the immobilisation and stabilisation of the heavy metals released from the mining sediments to the existing water.

2. Material and methods

2.1. Site description

Contaminated sediments were collected in Portman Bay, Murcia, Spain, (37°35'09.3"N, 0°50'53.5"W). Sampling took place on July 2017 and February 2018. Ten samples were obtained at 60-100 cm depth, in the unsaturated zone (above sea level). The samples were taken in the same area of the coastline where Alorda-Kleinglass et al. (2019) installed piezometers for water table characterisation. Results from those piezometers indicate that groundwater table was always below the sampling depth. At sampling depth, the studied yellow sediment has a major concentration of jarosite and it is abundant and representative of

Portman bay. Later, the studied sediment was covered with a dark brown sandy and permeable sediment, with a variable depth along the Portman Bay. In the Supplementary Materials section, Figure S1 shows the sampling area (Fig. S1b), the covered and studied sediments (Fig. S1c). In the Portman Bay border, the studied sediment can be found a few centimetres depth (Fig. S1d), which demonstrates the complexity of the studied area. Samples were taken inland at 5-10 meters from the coastline with the aim of evaluating the jarosite-sediment fraction susceptible to interact with infiltrated meteoric water.

Two different waste marble powders (WMP-1 and WMP-2) were sampled from two landfills employed by local marble industries in Novelda, Spain. The purpose of testing two different waste materials was to test the effectiveness of WMP with different levels of $CaCO_3$ in their composition. In addition, two commercial limes (Lime-1 and Lime-2), $Ca(OH)_2$, employed as a commercial construction material, were chosen for their chemical purity, yielding 5 cases (original sediment and 4 mixtures) to be analysed.

2.2. Sediment and precipitate characterisation

The phase composition of sediments and precipitates was analysed by powder X-ray diffraction (XRD) on a Bruker D8-Advance diffractometer with mirror Goebel (non-planar samples) using the CuKα radiation, a setting of 40 kV and 40 mA, 2q: 3–60, the step size of 0.05º and the scan step of 3s. XRD data were collected and interpreted using the XPowder software package, which allows the nonlinear least squares quantitative analysis for the phases identified and global amorphous stuff, overall from the database records. The qualitative search-matching procedure was based on the ICDD-PDF2 database (ICDD, 2003). The calculation of the global amorphous stuff considers that amorphous absorption contributes to the full-profile background and represents a percentage of amorphous phases in the sample (Martin Ramos, 2004). The presence of amorphous iron phases was evaluated combining Raman spectroscopy (FT-Raman Bruker RFS 100 operating at 1064nm) and the amorphous fraction obtained with XRD. Heavy metal concentration in sediments was measured with inductively coupled plasma mass spectrometry (ICP-MS, MS Analytical, Canada) after an acid digestion using a combination of hydrochloric, nitric, perchloric and hydrofluoric acids.

Field Emission Scanning Electron Microscope (FESEM, ZEISS Merlin VP Compact device) was used to characterise the precipitate forms and EDX (energy dispersive X-ray) was also applied to chemically analyse the elements associated with the FESEM images.

The colour of the solid bases, the original and treated sediments were estimated using the Munsell Soil Color Chart. Soil Color Charts offer an affordable way to evaluate and classify the colour of powdered solids. Munsell colour system is a colour space based on three properties of colour: hue, value (lightness), and chroma (colour purity).

The specific surface area (SSA) was determined by the nitrogen adsorption technique through the BET method (Rouquerol et al., 1994).

The particle size distribution was determined according to standard procedures (Gee and Or, 2002) and classified according to USDA (U.S. Department of Agriculture) criteria.

Cation exchange capacity (CEC) was measured in air dried and sieved (2 mm) samples following the so-called displacement after washing method (Rhoades, 1982). Sodium acetate was used as the saturation solution, then ethanol was used to wash the excess of saturation salt, and finally ammonium acetate solution was used to replace adsorbed cations, according to Sumner and Miller (1996).

2.3. Experiments: mixture experiments and lixiviation columns

2.3.1. Mixture experiments

Jarosite-rich sediments were mixed with the four different treatments, composed of two additions of waste marble powder (WMP-1 and WMP-2) and two additions of lime (Lime-1 and Lime-2). The employed mixture sediment:base ratios was 2:1. Mixtures of 50 g were obtained, and 50 g of deionised water were added to each mixture. The deionised water represents the meteoric water, which is always present in all the bay. Three replications were performed for each treatment and mixture ratio, and they all were preserved in 150 ml plastic containers (7.6 cm height and 5 cm diameter). Mixtures changed their colour and became consolidated in few hours (less than 24h). Then, they were dried in an oven at 40 ºC during 48h for mineralogical characterisation.

2.3.2. Lixiviation columns

Column experiments were developed to simulate the behaviour of passive treatments for remediation of acid mine drainage and to evaluate the reactivity of the original sediment and the mixtures with lime and WMP in contact with water. This static experiment aimed to determine the maximum amount of heavy metals that can leak from heavy-metal-bearing jarosite. This experiment simulates the interaction between water-sediment after water accumulations in the bay. We employed deionised water to evaluate the interaction between meteoric waters and the sediment/mixtures in the context of future passive treatments. Sediments are placed in the unsaturated zone above sea level and meteoric and superficial waters are more likely to react with treated sediments than with salty groundwater and seawater.

PVC columns of 73 cm height and 5 cm diameter were filled with mixtures of contaminated sediments and additions. Only mixtures with WMP-2 and Lime-2 additions were used because mixture experiments revealed those as the most effective treatments. All the columns were filled with 200 g of jarosite-rich sediments, 50 g of addition (relation 1:4) and 200 g of deionised water. Untreated sediments were tested in the same conditions although using 200 g of sediment and 150 g of deionized water. The bottom of each column contained a sand filter to prevent loss of fine particles from the sediments. A valve at the bottom of the column controls the water flux. Deionised water was added to the five cases and the resulting leachate was regularly sampled between 5 to 8 days. Between two consecutive sampling days, the valve remained closed and water had no movement inside the column. Sampling interval was long enough to let water in the column to fill all sediment pores and to let reactions take place in the complete domain of the column. Collected aqueous samples were analysed through pH measurement (Crison 25+ pH meter; ±0.01 accuracy) and ICP-MS analysis (VG PQ-ExCell, THERMO ELEMENTAL).

2.4. Geochemical modelling

The geochemical reactions of dissolution-precipitation and sorption were modelled with PHREEQC (*PH REdox EQuilibrium*) code using 3.4.0 version (Parkhurst and Appelo, 2013). PHREEQC calculates the saturation index, SI, as SI = log (IAP/K). IAP is the ion activity product and K is the equilibrium constant. The saturation index determines whether the water is saturated (equilibrium, SI = 0), undersaturated (mineral dissolution, SI < 0), or

supersaturated (mineral precipitation, SI > 0) with respect to the given mineral or phase. The geochemical reaction simulations involve two steps: (1) jarosite dissolution until reaching the saturation. To estimate the saturation state of the heavy metal phases, we considered that jarosite dissolution is produced in the lixiviated water from the sediment in contact with deionised water using the chemical composition obtained in the column experiment. (2) The addition of different moles of $CaCO_3$ and $Ca(OH)_2$ in different steps using the methodology described in Benavente et al., (2015), in isothermal conditions, through REACTION keyword. This keyword data block is used to define irreversible reactions that transfer specified amounts of elements to or from the aqueous solution during batch-reaction or transport calculations. Specific ion interaction theory is applied to estimate single-ion activity coefficients in electrolyte solutions using the Minteq.v4 thermodynamic database for the equilibrium constants.

Sorption reactions are modelled as surface complexation reactions of heavy metal ions on hydrous ferric oxide (Hfo), also referred to as ferrihydrite. The model uses the Gouy-Chapman equation to relate surface charge and potential, derived from Dzombak and Morel (1990). Ferrihydrite, like many other oxy-hydroxides, binds metals and protons on strong and weak sites and develops a charge depending on the ions sorbed. In our simulation, we will provide the concentration of adsorbed heavy metal on hydrous ferric oxide as the sum of adsorbed metals on strong and weak binding sites. Surface speciation has been performed at specified pH values fixed with NaOH (using “Fix_H+” keyword defined in PHASES data block). The composition and other characteristics of an assemblage of surfaces are defined with the SURFACE data block. We selected Minteq.v4 database that contains thermodynamic data for a diffuse-double-layer surface named Hfo.

Results and discussion

3.1. Mineralogical and geochemical characterisation of sediments and bases

Mineralogical composition of the studied samples was mainly identified and quantified using XRD (Fig. 1). The XRD pattern of sediments from Portman Bay showed a low signal-to-noise ratio comparing to studied bases (Fig. 1a).

The studied sediments are mainly composed of jarosite, quartz, phyllosilicates and siderite and, in a minor proportion, magnetite (Fig. 1). The fraction of amorphous phase is significant, mainly due to the presence of iron oxides, hydroxides and oxyhydroxides. The two most

important major elements are Fe and S, with a concentration of 32.4 and 7.7 % of the total weight respectively. The concentration of the heavy metals revealed the contaminated nature of the studied sediments, particularly the concentration of lead, zinc, arsenic, manganese and chromium (Table 1).

This geochemical and mineralogical composition is different to previous studies (Pérez-Sirvent et al., 2007; Martínez-Sánchez et al., 2008; Pérez-Sirvent et al., 2011; Pérez-Sirvent et al., 2016), which reflects the variability of the mining wastes and complexity of the studied area. Although XRD patterns of the sediment indicated an absence of characteristic peaks for heavy-metal-bearing minerals, they can be presented at small amounts (below of the detection limit of the XRD technique) as well as adsorbed or structurally incorporated into jarosite.

Waste marble powders present different mineralogical composition according to their source. WMP-1 consists of calcite, dolomite and quartz whereas WMP-2 only contains calcite and amorphous phase. The fraction of amorphous phase is scarce for both WMP (Table 2). The studied limes have different chemical purity. Lime-1 is composed of portlandite, calcite, C2S and quartz, and Lime-2 only presents portlandite and calcite (Table 2). The fraction of amorphous phase is important due to the presence of the analysed portlandite, which causes a broadening of the XRD peaks due to crystalline imperfections and other structural features (Sanjuán et al., 2019) (Fig.1).

According to the USDA criteria, the untreated sediment was a clear sand (99/1/0 for sand/silt/clay, respectively). WMP-1 and WMP-1 were classified as a silty clay material (0/58/42 and 1/74/25, respectively) whereas Lime-1 and Lime-2 presented a silty loam particle size distribution (14/79/7 and 15/57/28, respectively) with 100% of particles below 0.2 mm.

3.2. Evolution of sediments by mixture with alkaline treatments

Results highlight significant differences in the reaction between the jarosite-rich sediments and solid bases (Table 2). Thus, the addition of lime caused the precipitation of hematite, gypsum and calcite, whereas waste marble powders form iron carbonates (ankerite-siderite) and, in a minor amount, hematite (Figs. 1 and 2). The elimination of jarosite was almost complete for the treated sediment with Lime-2 because it has more concentration of portlandite than Lime-1. For waste marble powders, the reaction was uncompleted, remaining

more than 50% of jarosite in the treated sediment. Figures 3g and 3h show the dissolution forms on the jarosite surface although most of jarosite in the treated sediment with WMP remains. In the Supplementary Materials section, we provide the EDX spectra of FESEMs for solid phases in Figure 3 of the untreated and treated sediments, which highlights the complexity of the precipitated minerals.

The presence of amorphous oxides, hydroxides and oxyhydroxides was evaluated by the amorphous fraction obtained with XRD, Raman, CEC and N_2 adsorption characterisations, FESEM observations and colour variations. The amorphous fraction increased notably with the lime treatment in comparison to the carbonate mixture (Table 2).

The XRD patterns of the treated sediments also displayed a low signal-to-noise ratio, similarly to Portman Bay sediments (Fig. 1a). The poor quality of the XRD of the treated sediments indicates the abundance of amorphous oxides and oxyhydroxides. Amorphous solids lack of periodicity and atoms are randomly distributed; therefore, X-rays will be scattered leading to a large bump and high background through the XRD pattern. Contrary, crystalline minerals cause a discrete XRD pattern with high intensity and narrow peaks whereas amorphous precipitates act as a material with a diffuse XRD pattern as it occurs in the XRD patterns of the treated sediments (Fig. 1b). Raman spectra were in concordance with XRD analysis. They reflected the jarosite reduction and the formation of amorphous oxides and oxyhydroxides by the addition of treatments, mainly by the lime treatments. The formation of poorly crystalline iron compounds is characterised by broad bands (Fig. 2).

Iron oxides, hydroxides and oxyhydroxides have a considerable specific and reactive surface area compared to other minerals found in the studied samples (Langmuir, 1997). The lack of well-defined crystal structure as well as the amorphous form (Fig. 3) cause an important fraction of microporosity (Benjamin, 1983). SSA and CEC values notably increased with the lime treatment in comparison to the WMP treatment and the original jarosite-rich sediments. Tables 2 and 3 relate the evolution of SSA and the amorphous fraction obtained using XRD in the treated sediments and highlight the contribution of the amorphous oxides and oxyhydroxides to its reactive surface area.

Although Raman spectra strongly depend on the studied area of the sample, results corroborated the mineral composition obtained with XRD and showed an increase in the bands of related oxides, hydroxides and oxyhydroxides (Fig. 2) (Das and Hendry, 2011; Kerolli-Mustafa et al., 2013). Broad bands from 600-900 cm^{-1} are assigned to poorly or

microcrystalline oxyhydroxides similar to ferrihydrite characterised in Das and Hendry (2011).

The colour evolution of the treated sediments reflects the mineralogical changes on Fe-minerals and confirmed the formation of iron oxides, hydroxides and oxyhydroxides. The colour of iron phases ranges gradually from yellow to dark-brown through black, depending on the degree of hydration, particle size and shape, and crystal structure (Chesworth et al., 2008). The original Portman sediment was yellow (5Y 7/6). The addition of both waste marble powders caused a light-yellow mixture (5Y 7/3) and therefore it slightly varied the original sediment colour. However, the addition of lime reddened the original sediment. Lime-sediment mixtures were bright reddish brown, although Lime-2 had the Chroma value (more reddish) higher (5YR 5/8) than Lime-1 (5YR 5/6). Colour evolution is in concordance with the increase of amorphous fraction obtained using XRD, CEC and SSA, particularly for lime mixtures (Tables 2 and 3) and amorphous fraction obtained using XRD in the treated sediments.

3.3. Lixiviation columns

Table 4 shows the reactivity of the original sediment and the mixtures Lime-2 and WMP-2 in contact with water. When water flowed through the sediment, heavy metal concentration increased by the dissolution of heavy-metal-bearing minerals (jarosite family and heavy metal minerals) as well as by ion-exchange reactions in minerals. These results demonstrate the potential toxicity of the sediment when it interacts with water. However, the concentration of the heavy metals in the lixiviated water with the contaminated sediment is small compared to their original concentration in the sediment. For example, concentrations of Pb, Zn, As, and Mn in the sediment were respectively 3955, 2018, 1664 and 1966 mg kg^{-1} whereas their peak concentrations in the lixiviated water were 0.05, 18.23, 0.03 and 11.01 mg kg^{-1}, respectively (Table 4).

Both treatments Lime-2 and WMP-2 reduced the mobilisation of the heavy metals from the sediment. However, heavy metal immobilisation with lime treatment was significantly more effective than WMP treatment in reducing concentrations of soluble and ion-exchangeable metal (Table 3). The reactive or neutralising component in the lime is portlandite ($Ca(OH)_2$) whereas WMP is calcite ($CaCO_3$). The enhanced effectiveness of $Ca(OH)_2$ compared to $CaCO_3$ was predominantly attributable to the higher initial sediment pH >9 (Table 4) with the

former treatment, which contributed to reduce trace metal mobility by adsorption, co-precipitation, encapsulation and amorphous iron minerals (Langmuir, 1997; Smith et al., 2006; Stoffregen, 1993; Stoffregen et al., 2000).

Metals oxyhydroxides are amphoteric phases and they become more soluble at low and high pH's (Langmuir, 1997). pH values in the column experiments were similar for untreated sediment (5.8-7.0) and treated with WMP (6.5-7.4) whereas pH of the treated sediment with lime reaches higher values (8.5-9.0). This behaviour might limit the use of lime for the sediment remediation and the lime dose should be carefully chosen to obtain pH<9.

Heavy metal stabilisation depends on the element although it can be considered effective after 15 days of experiment, especially for Zn, Cd, Pb and Mn. Both treatments did not benefit the stabilisation of Cr and Ni, although these heavy metals presented a low concentration in the sediment (Table 1).

However, arsenic behaved differently. Although its concentration in the lixiviated water from both original and treated WMP-2 sediments was low, its concentration in Lime-2 treatment was higher than in the original (Table 4), contrarily to the rest of the analysed heavy metals. This discrepancy can be attributed to the sorption reactions and its dependence with pH of As(V), the more stable arsenic aqueous phase in our oxidizing experimental conditions. Williams et al. (2003) concluded that from pH 3 to 7 the percentage of adsorbed As(V) decreases slightly from approximately 95 to 85%. As the pH increases from 7 to 10, the percentage of As(V) adsorbed drops dramatically, decreasing to approximately 40 to 50% between pH 9 and 10. This behaviour is typical of anion adsorption onto variably charged surfaces and results from the pH-dependent surface charge and aqueous speciation of As(V). For pH $\leq$ 7 (in original and WMP treated sediments), As(V) exists predominately as $H_2AsO_4^-$ and is attracted to positively charged sediment surfaces (e.g., Fe oxides). At high pH values (in lime treated sediments), As(V) exists as an anion in the form $HAsO_4^{2-}$ and the Fe oxide surfaces become increasingly negatively charged. The repelling negative charges between the sediment particle and the As(V) ion help to explain the decrease in As(V) adsorption with an increase in pH. These results indicate that pH would have a very strong effect on As(V) water concentration and transport, with a decreasing of the adsorption capacity by almost one order of magnitude in moving from approximately pH 7 to 9.

The reactivity of this type of jarosite-rich sediments will lead to serious problems for the environment if they are exposed to waters. In particular, in Portman Bay, the connexion

between sediments and seawater causes a dramatic effect on the ecotoxicological and human health. Alorda-Kleinglass et al. (2019) investigated the contribution of the remobilisation and transfer of dissolved metals from the mine tailing deposits to the coastal waters (both submarine groundwaters and porewaters) of Portman Bay. They concluded that concentrations of dissolved metals in coastal waters are important, although they are significantly reduced by the presence of dissolved iron that acts as a geochemical barrier and by the co-precipitation of dissolved metals with iron hydroxides supplied by submarine groundwater discharges.

3.4. Geochemical modelling

The final pH of lixiviates from treated sediments (Table 4) and their chemical composition varied with each treatment. The lixiviate for the WMP mixture presented a neutral pH value, with a chemical composition rich in Ca^{2+} and HCO_3^-. However, lime mixture reached alkaline pH conditions and the chemical composition of the resulting water contained Ca^{+2} and OH^-. These conditions caused different reaction pathways between jarosite and solid bases that lead to a specific mineralogical composition of treated sediment as well as metal retention characteristics.

The geochemical simulations of dissolution-precipitation considered (1) that jarosite dissolution was produced in the lixiviated water from the sediment (Table 4); and (2) the addition of $CaCO_3$ and $Ca(OH)_2$ for the treatments with WMP and lime, respectively. Results from PHREEQC simulations estimated that the lixiviate for the WMP mixture was supersaturated in ankerite-siderite (Fig. 4), although only ankerite (iron-bearing dolomite) was detected with XRD in the mixture experiment (Table 2). For the lime treatment, the theoretical pore water had an alkaline pH value and it was supersaturated in gypsum and siderite (Fig. 4). In the mixture experiment (Table 2), we detected gypsum in both lime treatments whereas siderite only was found in the Lime-2 mixture. Both WMP and lime treatments were supersaturated in iron oxides, hydroxides and oxyhydroxides minerals and amorphous phases non-detectable by the employed techniques. In PHREEQC calculations, we used iron oxides, hydroxides and oxyhydroxides that potentially can precipitate from the lixiviated water, which include the following minerals and amorphous (am) phases: for oxides: Hematite-Fe_2O_3, Maghemite Fe_2O_3; for hydroxides: Ferrihydrite-$Fe(OH)_3$, $Fe(OH)_3$(am); and for oxyhydroxides: Goethite-FeOOH, Lepidocrocite-FeOOH.

We also evaluated the saturation stage evolution of the heavy metals phases that potentially can be presented in the lixiviated water of the treated sediment: $Cr(OH)_3(am)$, $Cr(OH)_3$, $Ni(OH)_2$, $Cu(OH)_2$, Zincite-ZnO, $Zn(OH)_2$, $Zn(OH)_2(am)$, $Zn(OH)_2(beta)$, $Cd(OH)_2(am)$, $Cd(OH)_2$, $CdSO_4 \cdot H_2O$, $FeAsO_4 \cdot 2H_2O$,$Zn_3(AsO_4)_2 \cdot 2.5H_2O$, $Pb_3(AsO_4)_2$, $Cu_3(AsO_4)_2 \cdot 2H_2O$, $Mn_3(AsO_4)_2 \cdot 8H_2O$, Bixbyite- Mn_2O_3, Hausmannite- Mn_3O_4, Manganite- MnOOH, Pyrochroite- $Mn(OH)_2$, Pyrolusite- MnO_2, Anglesite- $PbSO_4$, Cerrusite- $PbCO_3$, Hydrocerrusite- $Pb_3(OH)_2(CO_3)_2$, $Pb(OH)_2$.

The evolution of the saturation index of the studied heavy metal phases is similar in both treatments, although the addition of lime reaches higher saturation index values (Fig. 4). For both treatments, Cd, Ni and As phases are undersaturated and they cannot be removed from lixiviated waters by precipitation, particularly in arsenates where the saturation index is sensitive to pH variations. However, most of the Zn, Mn, Cu, Cr and Pb phases are supersaturated, particularly for the lime treatment, which indicates that they also can be removed by co-precipitation with iron precipitates.

Iron oxides, hydroxides and oxyhydroxides minerals are more stable thermodynamically than amorphous phases, but short-term kinetics reasons explain the metastable existence of hydrated, poorly crystalline iron oxides, hydroxides and oxyhydroxides phases in treated mixtures. According to Gay-Lussac-Ostwald or Ostwald step rule, the nucleation of a more soluble phase (such as amorphous or a metastable phase) is kinetically favoured over less soluble analogues (such as calcite) because of the lower interfacial energy (and thus lower nucleation energy) between minerals and water (Langmuir, 1997). This process was enhanced in our study because pH in the lixiviate increases and amorphous iron oxides, hydroxides and oxyhydroxides become more supersaturated. As the supersaturation of the solution is sufficiently high, the amorphous phases suffer rapid nucleation that may lead to the precipitation of low crystallinity and amorphous forms (Fig. 3).

Lime treatment forms more amorphous phases with reactive surface areas (Table 3) that can also remove heavy metals by sorption reactions. Sorption of heavy metals comprises a whole suite of reactions ranging from adsorption to solid solution and mineral precipitation and they may be sequential depending on the geochemical environment. Often there is an initial fast adsorption step followed by a slow step where the adsorbed species are incorporated into the crystal structure to form a solid solution (Appelo and Postma, 2005).

Sorption of heavy metals on amorphous iron oxyhydroxide varies with pH as its surface becomes protonated or deprotonated as a function of pH. All metals show low sorption at low pH and increased sorption as pH increases, consistent with the amphoteric behaviour of the oxide or hydroxide (Langmuir, 1997; Appelo and Postma, 2005). Figure 5 depicts the variation of concentration of heavy metal in the solution and on the hydrous ferric oxide at different pH values calculated using PHREEQC. Adsorption sites on hydrous ferric oxide are termed Hfo_ (e.g.: Hfo_OPb^{+} for Pb^{2+} sorbed on the hydrous ferric oxide, Hfo) and it is given by the sum of strong and weak binding sites. We did not include the calculations for Cr due to the lack of conscience in the databases. Cr presents the lowest concentration in the lixiviated water (Table 4) and the estimation of the sorption process of heavy metals by the amorphous amorphous oxides and oxyhydroxides is not affected.

The sorptive abilities of minerals are proportional to their surface areas. We modelled the sorption process using the specific surface area of treated sediment (Table 3). For these specific surface area values, the concentration of heavy metal on the hydrous ferric oxide for both treatments were similar and therefore Figure 5 does not differentiate between them. For example, for a pH=7 Hfo_OPb^{+} is $1.705 \cdot 10^{-6}$ m and $1.689 \cdot 10^{-6}$ m for a specific surface area of 36.06 $m^2\ g^{-1}$ (lime) and 7.86 $m^2\ g^{-1}$ (WMP), respectively.

Cu and Pb present the maximum concentration on the hydrous ferric oxide (Fig. 5a). Sorbed concentrations of Cd and Ni increase as increases pH and become more concentrated than in the solution for pH>9 (Fig. 5a). Mn and Zn concentration in the solution is higher than sorbed on the hydrous ferric oxide (Fig. 5b). Adsorption affinity of different metal cations obeys the following tendency according to Irving-Williams (1959) series:

Pb > Cu > Cd > Ni> Zn >Mn > Ca

Sorption process is therefore expected for Pb and Cu due to its strong affinity for binding sites at low pH values and also to their low concentrations (Table 4). Pb can occupy binding sites without reaching concentrations where Pb-bearing minerals are supersaturated (Fig. 4). However, the initial Cu concentration in lixiviate waters is important and its concentration on the surface may lead to mineral precipitation. Consequently, Pb and Cu may occupy most of the sorption sites and limit the sorption process for the rest of the heavy metals, which are more concentrated in the initial lixiviate waters than Pb and Cu. Other species highly concentrated as Ca^{2+} from the treatments may also compete by sorption sites and decrease the sorption process. Cd and Ni sorption may be important comparatively to precipitation process

for pH>9 in the lime treatment, whereas the sorption process for Mn and Zn will be scarcer compared to mineral precipitation. Mn and Zn present the highest concentration in lixiviate waters and reach high supersaturation values (Fig. 4).

In the previous section, we discussed that treatments do not stabilize arsenic in the lixiviate waters because of sorption reactions of As(V) dependent on pH (Fig. 5b). Arsenate will be attracted to positively charged surfaces and repelled from negative surfaces and so will exhibit high sorption at low pH and low sorption at high pH (Appelo and Postma, 2005). Consequently, As cannot be removed from the lixiviated waters by co-precipitation nor sorption reaction, which explains the increment of As in the lixiviated waters of the treated sediment compared to the untreated sediment.

Figures 5 and 6 also highlight the amphoteric behaviour of As, Cr, Cu, and Zn phases, being negligible for Fe, Ni, Cd, Pb, and Mn phases. This behaviour can be related to the decline of the saturation index for pH>9 in lime treatment and pH>8 in WMP treatment.

The effectiveness in the heavy metal stabilisation by lime is due to basic pH values that can be reached. This chemical environment leads to the precipitation of more stable phases in form of oxides, hydroxides and oxyhydroxides, which sorbs and co-precipitates considerable amounts of potentially toxic elements. Langmuir (1997) argued that due to their low concentrations of heavy metals in waters it is difficult to distinguish whether the concentration of heavy metal on the solid is due to adsorption or is due to the formation of a particular solid solution and precipitation or both processes. According to the geochemical modelling (Figs. 4 and 5) and the reduction of heavy metals by the treatments (Table 4), Zn and Mn, that present the highest values of concentration, are expected to be stabilized mainly by precipitation, and Cu, Pb and Cd by both precipitation and sorption. Ni and Cr do not undergo a significative reduction in the lixiviated water and As on the contrary, increases its concentration in the treated sediment.

Finally, the gypsum precipitation in the lime treatment produces an interparticle pore clogging that reduces the hydraulic conductivity of the remediated sediment, and consequently, the water-sediment interaction after the sediment treatment.

4. Conclusions

We have studied jarosite-rich sediments from Portman Bay, one of the most contaminated points in the Mediterranean Sea by mining-metallurgical activities. Our results revealed that

the precipitation of iron oxides, hydroxides and oxyhydroxides in the treated jarosite-rich sediments as result of the proposed treatments play a critical role in the immobilisation of heavy metals. These iron phases sorb and co-precipitate considerable trace metals, decreasing their mobility and potential bioavailability. Iron phases were mostly found in the amorphous fraction and they presented a large specific surface area and cation-exchange capacity that enhances their superficial reactivity. These phases precipitated from the jarosite dissolution reached high supersaturation values and formed within a few hours (less than 24h). Lime was more effective, than waste marble powder, especially for Zn, Cd, and Mn where lime reduces more than 95% of their concentration in the lixiviated water. PHREEQC calculations also showed that most of the Zn, Mn, Cr, Cu and Pb phases are supersaturated (Fig. 4), particularly for the lime treatment, indicating that they can be removed by co-precipitation with iron precipitates. Particularly, Cu, Pb and Cd (Fig. 5a) present strong sorption on amorphous iron oxyhydroxides and their removal are caused by a combination of precipitation and sorption processes. Both Lime-2 and WMP-2 treatments did not benefit the stabilisation of Cr and Ni, although their concentration in the sediment was low. Contrarily, As concentration in lime treatment was higher than in the untreated and WMP-treated sediment due to amphoteric behaviour and sorption reactions that depend on pH.

The heavy metal concentration in lixiviates from both the original and the treated sediments was controlled by the jarosite solubility, the pH and the interaction between these two factors. Higher levels of $Ca(OH)_2$ in lime and its higher reactivity compared to $CaCO_3$ mostly explain the better performance of lime versus waste marble powder. Lime is a worldwide accessible construction material, and its higher reactivity permits a reduction in the required quantities. However, due to the amphoteric behaviour of some heavy metal phases, the pH of the mixture should remain below 9. Another weakness of using lime is the increase in the concentration of As. Although lime is more effective than waste marble powder in metal immobilisation for the studied Portman sediment, the use of this industrial sub-product presents a substantial environmental benefit and lower cost, and consequently, it should also be considered as a soft treatment in contaminated-soil remediation.

As a consequence, the movement of sediments to another site would involve a change in the potential mobility of the associated metals. The high reactivity of jarosite with high amounts of heavy metals would give rise to a serious risk if they were moved, particularly if they reached a location well-connected to meteoric waters. In such a case, an important amount of heavy metals could be released, with severe consequences to the environment.

Acknowledgements

This study was funded by the University of Alicante [GRE17-12 from] and the Spanish Government [grant number RTI2018-099052-B-I00]. Additional acknowledge to the Technical Research Services of the University of Alicante (SSTTI-UA) for the analyses performed using the equipment held at this institution, which was financed by the EU, MINECO and Generalitat Valenciana [State Programme for Knowledge Generation and Scientific and Technological Strengthening of the R+D+i System and P.O. FEDER 2007-2013 funds].

571 **References**

572 Acero, P., Ayora, C., Carrera, J., 2007. Coupled thermal, hydraulic and geochemical
573 evolution of pyritic tailings in unsaturated column experiments. Geochim.
574 Cosmochim. Acta, 71(22): 5325-5338. DOI:10.1016/j.gca.2007.09.007
575 Alorda-Kleinglass, A., Garcia-Orellana, J., Rodellas, V., Cerdà-Domènech, M., Tovar-
576 Sánchez, A., Diego-Feliu, M., Trezzi, G., Sánchez-Quilez, D., Sanchez-Vidal, A.,
577 Canals, M., 2019. Remobilization of dissolved metals from a coastal mine tailing
578 deposit driven by groundwater discharge and porewater exchange. Sci. Total
579 Environ., 688: 1359-1372. DOI:10.1016/j.scitotenv.2019.06.224
580 Appelo, C. A. J., Postma, D. 1993. Geochemistry, groundwater and pollution. Rotterdam:
581 A.A. Balkema.
582 Bangira, C., Loeppert, R.H., Moore, T.J., Hons, F.M., Shahandeh, H., 2017. Relative
583 effectiveness of CaCO3 and Ca(OH)2 in minimizing metals solubility in
584 contaminated sediment. J. Soils Sed., 17(6): 1796-1805. DOI:10.1007/s11368-016-
585 1641-9
586 Ben Hamed, S., Guardiola, F., Cuesta, A., Martínez, S., Martínez-Sánchez, M.J., Pérez-
587 Sirvent, C., Esteban, M.Á., 2017. Head kidney, liver and skin histopathology and
588 gene expression in gilthead seabream (Sparus aurata L.) exposed to highly polluted
589 marine sediments from Portman Bay (Spain). Chemosphere, 174: 563-571.
590 DOI:10.1016/j.chemosphere.2017.02.009
591 Benjamin, M.M., 1983. Adsorption and Surface Precipitation of Metals on Amorphous Iron
592 Oxyhydroxide. Environ. Sci. Technol., 17(11): 686-692. DOI:10.1021/es00117a012
593 Cesar, A., Marín, A., Marin-Guirao, L., Vita, R., Lloret, J., Del Valls, T.A., 2009. Integrative
594 ecotoxicological assessment of sediment in Portmán Bay (southeast Spain).
595 Ecotoxicol. Environ. Saf., 72(7): 1832-1841. DOI:10.1016/j.ecoenv.2008.12.001
596 Chesworth W., Perez□Alberti A., Arnaud E., Morel□Seytoux H.J., Morel□Seytoux H.J.,
597 Schwertmann U. (2008) Iron oxides. In: Chesworth W. (eds) Encyclopedia of Soil
598 Science. Encyclopedia of Earth Sciences Series. Springer, Dordrecht
599 Conesa, H.M., Schulin, R., 2010. The Cartagena-La Unión mining district (SE spain): A
600 review of environmental problems and emerging phytoremediation solutions after
601 fifteen years research. J. Environ. Monit., 12(6): 1225-1233. DOI:10.1039/c000346h

602 Das, S., Hendry, M.J., 2011. Application of Raman spectroscopy to identify iron minerals
603 commonly found in mine wastes. Chem. Geol., 290(3-4): 101-108.
604 DOI:10.1016/j.chemgeo.2011.09.001
605 Domènech, C., Ayora, C., De Pablo, J., 2002. Sludge weathering and mobility of
606 contaminants in soil affected by the Aznalcollar tailing dam spill (SW Spain). Chem.
607 Geol., 190(1-4): 355-370. DOI:10.1016/S0009-2541(02)00125-0
608 Durães, N., Bobos, I., da Silva, E.F., 2017. Speciation and precipitation of heavy metals in
609 high-metal and high-acid mine waters from the Iberian Pyrite Belt (Portugal).
610 Environ. Sci. Pollut. Res., 24(5): 4562-4576. DOI:10.1007/s11356-016-8161-4
611 Dutrizac, J.E., Dinardo, O., Kaiman, S., 1980. Factors affecting lead jarosite formation.
612 Hydrometallurgy, 5(4): 305-324. DOI:10.1016/0304-386X(80)90022-5
613 Dutrizac, J.E., Hardy, D.J., Chen, T.T., 1996. The behaviour of cadmium during jarosite
614 precipitation. Hydrometallurgy, 41(2-3): 269-285.
615 Dutrizac, J.E., Jambor, J.L., 2000. Jarosites and their application in hydrometallurgy,
616 Reviews in Mineralogy and Geochemistry, pp. 404-452.
617 Dutrizac, J.E., Jambor, J.L., Chen, T.T., 1987. The behaviour of arsenic during jarosite
618 precipitation: Reactions at 150°c and the mechanism of arsenic precipitation. Can
619 Metall Q, 26(2): 103-115. DOI:10.1179/cmq.1987.26.2.103
620 Dzombak, D.A. and Morel, F.M.M., 1990. Surface complexation modeling: hydrous ferric
621 oxide. Wiley and Sons, New York, 393 pp.
622 García-Lorenzo, M.L., Martínez-Sánchez, M.J., Pérez-Sirvent, C., Agudo, I., Recio, C., 2014.
623 Isotope geochemistry of waters affected by mining activities in Sierra Minera and
624 Portman Bay (SE, Spain). Appl. Geochem., 51: 139-147.
625 DOI:10.1016/j.apgeochem.2014.10.002
626 Gasharova, B., Göttlicher, J., Becker, U., 2005. Dissolution at the surface of jarosite: An in
627 situ AFM study. Chem. Geol., 215(1-4 SPEC. ISS.): 499-516.
628 DOI:10.1016/j.chemgeo.2004.06.054
629 Gee G W, Or D. 2002. Particle-size analysis. In Dane J, Topp C, (eds.) Methods of soil
630 analysis part 4 physical methods. Soil Science Society of America, Madison, WI,
631 USA.
632 González-Ibarra, A.A., Nava-Alonso, F., Fuentes-Aceituno, J.C., Uribe-Salas, A., 2016.
633 Hydrothermal decomposition of industrial jarosite in alkaline media: The rate
634 determining step of the process kinetics. J. Min. Metall. Sect. B Metall., 52(2): 135-
635 142. DOI:10.2298/JMMB150430016G

636 Gunneriusson, L., Sandström, Å., Holmgren, A., Kuzmann, E., Kovacs, K., Vértes, A., 2009.
637 Jarosite inclusion of fluoride and its potential significance to bioleaching of sulphide
638 minerals. Hydrometallurgy, 96(1-2): 108-116. DOI:10.1016/j.hydromet.2008.08.012
639 Hudson-Edwards, K.A., Schell, C., Macklin, M.G., 1999. Mineralogy and geochemistry of
640 alluvium contaminated by metal mining in the Rio Tinto area, southwest Spain. Appl.
641 Geochem., 14(8): 1015-1030. DOI:10.1016/S0883-2927(99)00008-6
642 ICDD (2003) International Centre for Diffraction Data. Campus Boulevard. Pennsylvania.
643 Powder Diffraction File, Rel. 2003
644 Irving, H. M. N. H., Williams, R. J. P., 1953. The stability of transition-metal complexes. J.
645 Chem. Soc.: 3192–3210. doi:10.1039/JR9530003192.
646 Kerolli-Mustafa, M., Bačič, I., Ćurkovič, L., 2013. Investigation of jarosite process tailing
647 waste by means of raman and infrared spectroscopy. Mater.wis. Werkstofftech.,
648 44(9): 768-773. DOI:10.1002/mawe.201300172
649 Langmuir, D., 1997. Aqueous Environmental Geochemistry. Prentice Hall, California, 600
650 pp.
651 Macías, F., Caraballo, M.A., Nieto, J.M., Rötting, T.S., Ayora, C., 2012. Natural pretreatment
652 and passive remediation of highly polluted acid mine drainage. J. Environ. Manage.,
653 104: 93-100. DOI:10.1016/j.jenvman.2012.03.027
654 Manteca, J.I., García, J.Á.L., Oyarzun, R., Carmona, C., 2014. The beach placer iron deposit
655 of Portman Bay, Murcia, SE Spain: The result of 33 years of tailings disposal (1957–
656 1990) to the Mediterranean seaside. Miner. Deposita, 49(6): 777-783.
657 DOI:10.1007/s00126-014-0511-x
658 Martin Ramos, J.D., 2004. Using XPowder: A software package for Powder X-Ray
659 diffraction analysis.
660 Martínez-Sánchez, M.J., Navarro, M.C., Pérez-Sirvent, C., Marimón, J., Vidal, J., García-
661 Lorenzo, M.L., Bech, J., 2008. Assessment of the mobility of metals in a mining-
662 impacted coastal area (Spain, Western Mediterranean). J. Geochem. Explor., 96(2-3):
663 171-182. DOI:10.1016/j.gexplo.2007.04.006
664 Mireles, I., Reyes, I.A., Flores, V.H., Patiño, F., Flores, M.U., Reyes, M., Acosta, M., Cruz,
665 R., Gutiérrez, E.J., 2016. Kinetic analysis of the decomposition of the KFe3 (SO4)2-x
666 (CrO4)x (OH)6 jarosite solid solution in Ca(OH)2 medium. J. Braz. Chem. Soc.,
667 27(6): 1014-1025. DOI:10.5935/0103-5053.20150357
668 Orozco, J.M.M., Huete, F.V., Alonzo, S.G., 1993. Environmental problems and proposals to
669 reclaim the areas affected by mining exploitations in the Cartagena mountains

(southeast Spain). Landsc. Urban Plann., 23(3-4): 195-207. DOI:10.1016/0169-2046(93)90068-O

Parkhurst, D.L., Appelo, C.A.J., 2013. Description of input and examples for PHREEQC version 3—A computer program for speciation, Batch-Reaction, One-Dimensional Transport, and Inverse Geochemical Calculations. In: Survey, U.G., Interior, U.D.o.t. (Eds.), U.S. Geological Survey Techniques and Methods, book 6, chap. A43. US Geological Survey, Denver CO (USA), pp. 497.

Patiño, F., Cruells, M., Roca, A., Salinas, E., Pérez, M., 2003. Kinetics of alkaline decomposition and cyanidation of argentian ammonium jarosite in lime medium. Hydrometallurgy, 70(1-3): 153-161. DOI:10.1016/S0304-386X(03)00074-4

Patiño, F., Reyes, I.A., Flores, M.U., Pandiyan, T., Roca, A., Reyes, M., Hernández, J., 2013. Kinetic modeling and experimental design of the sodium arsenojarosite decomposition in alkaline media: Implications. Hydrometallurgy, 137: 115-125. DOI:10.1016/j.hydromet.2013.05.005

Patiño, F., Salinas, E., Cruells, M., Roca, A., 1998. Alkaline decomposition-cyanidation kinetics of argentian natrojarosite. Hydrometallurgy, 49(3): 323-336.

Pérez-Sirvent, C., García-Lorenzo, M.L., Hernández-Pérez, C., Martínez-Sánchez, M.J., 2018. Assessment of potentially toxic element contamination in soils from Portman Bay (SE, Spain). J. Soils Sed., 18(6): 2248-2258. DOI:10.1007/s11368-017-1756-7

Pérez-Sirvent, C., García-Lorenzo, M.L., Martínez-Sánchez, M.J., Molina-Ruiz, J., Marimon, J., Navarro, M.C., 2011. Use of marble cutting sludges for remediating soils and sediments contaminated by heavy metals. Environ Prog Sustainable Energy, 30(4): 533-539. DOI:10.1002/ep.10502

Pérez-Sirvent, C., García-Lorenzo, M.L., Martínez-Sánchez, M.J., Navarro, M.C., Marimón, J., Bech, J., 2007. Metal-contaminated soil remediation by using sludges of the marble industry: Toxicological evaluation. Environ. Int., 33(4): 502-504. DOI:10.1016/j.envint.2006.11.003

Pérez-Sirvent, C., Hernández-Pérez, C., Martínez-Sánchez, M.J., García-Lorenzo, M.L., Bech, J., 2016. Geochemical characterisation of surface waters, topsoils and efflorescences in a historic metal-mining area in Spain. J. Soils Sed., 16(4): 1238-1252. DOI:10.1007/s11368-015-1141-3

Perez-Sirvent, C., Martínez-Sánchez, M., García-Lorenzo, M.L., Hernández-Córdoba, M., Molina-Ruiz, J., Martinez, S., Gonzalez, E., Pérez-Espinosa, V., 2014. A Preliminary Zonation to Support the Remediation and the Risk Assessment of an Area

Contaminated by Potentially Toxic Elements in Murcia Region (SE, Spain). Procedia Earth and Planetary Science, 10: 388-391. DOI:10.1016/j.proeps.2014.08.069

Qian, G., Fan, R., Short, M.D., Schumann, R.C., Li, J., Li, Y., Smart, R.S.C., Gerson, A.R., 2019. Evaluation of the rate of dissolution of secondary sulfate minerals for effective acid and metalliferous drainage mitigation. Chem. Geol., 504: 14-27. DOI:10.1016/j.chemgeo.2018.12.003

Rhoades, J.D., 1982. Cation Exchange Capacity. In: *Methods of soil analysis, Part 2. Chemical and Microbiological properties, 2nd edition.* Ed: A.L. Page, R.H. Miller, D.R. Keeney. ASA and SSSA. (Madison , WI-USA)

Roca, A., Cruells, M., Patiño, F., Rivera, I., Plata, M., 2006. Kinetic model for the cyanidation of silver ammonium jarosite in NaOH medium. Hydrometallurgy, 81(1): 15-23. DOI:10.1016/j.hydromet.2005.09.004

Roca, A., Patiño, F., Viñals, J., Núñez, C., 1993. Alkaline decomposition-cyanidation kinetics of argentojarosite. Hydrometallurgy, 33(3): 341-357. DOI:10.1016/0304-386X(93)90071-K

Rose, S., Elliott, W.C., 2000. The effects of pH regulation upon the release of sulfate from ferric precipitates formed in acid mine drainage. Appl. Geochem., 15(1): 27-34. DOI:10.1016/S0883-2927(99)00015-3

Rouquerol, J., Avnir, D., Everett, D.H., Fairbridge, C., Haynes, M., Pernicone, N., Ramsay, J.D.F., Sing, K.S.W., Unger, K.K., 1994. Guidelines for the Characterization of Porous Solids, Studies in Surface Science and Catalysis, pp. 1-9. DOI:10.1016/S0167-2991(08)63059-1

Salinas, E., Roca, A., Cruells, M., Patio, F., Córdoba, D.A., 2001. Characterization and alkaline decomposition-cyanidation kinetics of industrial ammonium jarosite in NaOH media. Hydrometallurgy, 60(3): 237-246. DOI:10.1016/S0304-386X(01)00149-9

Sanjuán, I., Benavente, D., Expósito, E., Montiel, V., 2019. Electrochemical water softening: Influence of water composition on the precipitation behaviour. Sep. Purif. Technol., 211: 857-865. DOI:10.1016/j.seppur.2018.10.044

Simón, M., Martín, F., García, I., Bouza, P., Dorronsoro, C., Aguilar, J., 2005. Interaction of limestone grains and acidic solutions from the oxidation of pyrite tailings. Environ. Pollut., 135(1): 65-72. DOI:10.1016/j.envpol.2004.10.013

Smith, A.M.L., Hudson-Edwards, K.A., Dubbin, W.E., Wright, K., 2006. Dissolution of jarosite [KFe3(SO4)2 (OH)6] at pH 2 and 8: Insights from batch experiments and

738 computational modelling. Geochim. Cosmochim. Acta, 70(3): 608-621.
739 DOI:10.1016/j.gca.2005.09.024
740 Soler, J.M., Boi, M., Mogollón, J.L., Cama, J., Ayora, C., Nico, P.S., Tamura, N., Kunz, M.,
741 2008. The passivation of calcite by acid mine water. Column experiments with ferric
742 sulfate and ferric chloride solutions at pH 2. Appl. Geochem., 23(12): 3579-3588.
743 DOI:10.1016/j.apgeochem.2008.08.011
744 Stoffregen, R.E., 1993. Stability relations of jarosite and natrojarosite at 150-250°C.
745 Geochim. Cosmochim. Acta, 57(11): 2417-2429. DOI:10.1016/0016-7037(93)90406-
746 M
747 Stoffregen, R.E., Alpers, C.N., Jambor, J.L., 2000. Alunite-jarosite crystallography,
748 thermodynamics, and geochronology, Reviews in Mineralogy and Geochemistry.
749 Mineralogical Society of America, pp. 453-479. DOI:10.2138/rmg.2000.40.9
750 Tang, L., Tang, C., Xiao, J., Zeng, P., Tang, M., 2018. A cleaner process for valuable metals
751 recovery from hydrometallurgical zinc residue. J. Clean. Prod., 201: 764-773.
752 DOI:10.1016/j.jclepro.2018.08.096
753 Wang, Y.M., Chen, T.C., Yeh, K.J., Shue, M.F., 2001. Stabilization of an elevated heavy
754 metal contaminated site. J. Hazard. Mater., 88(1): 63-74. DOI:10.1016/S0304-
755 3894(01)00289-8
756

Table 1. Concentration (mg kg^{-1}) of the heavy metals in the studied sediment.

Element	Cr	Ni	Cu	Zn	As	Cd	Pb	Mn
mg kg^{-1}	14.0	6.7	37.8	2018	1664	2.1	3955	1967

Table 2. Mineralogical composition of the original and treated sediments with waste marble powders (WMP-1 and WMP-2) and lime (Lime-1 and Lime-2). Jar: jarosite; Sider: Siderite; Mag: magnetite; Hem: Hematite; Ank: Ankerite; Cal: calcite; Dol: dolomite; Por: Portlandite; Gym: gypsum; Q: quartz; Mos: muscovite; C2S: Larnite; Amo: amorphous phase.

	Sample	Jar	Sider	Mag	Hem	Ank	Cal	Dol	Por	Gyp	Q	Mus	C2S	Amo
Original	**Sediment**	45	8	6							11	10		20
	Lime-1						15		28		3		40	14
	Lime-2						30		60					10
	WMP-1						60	32			2			6
	WMP-2						96							4
Treated	**Lime-1**	10			6		26			21	6	6		25
	Lime-2		3		4		38			30	4	5		16
	WMP-1	26			2	19	42				2			9
	WMP-2	33			1	8	53							5

Table 3. Specific surface area (SSA) and cation-exchange capacity (CEC) of the original and treated sediments with waste marble powders (WMP-1 and WMP-2) and lime (Lime-1 and Lime-2).

Sample	SSA (m^2 g^{-1})	CEC (meq/100 solid)
Sediment	11.25	3.54
Mix Lime-1	43.89	18.58
Mix Lime-2	36.06	17.43
Mix WMP-1	8.56	2.86
Mix WMP-2	7.86	2.79

Table 4. pH and concentration (μg L^{-1}) of the heavy metals in the lixiviated waters from the original and treated sediments with Lime-2 and WMP-2 in the lixiviation columns.

Sample	pH	Fe	Cr	Ni	Cu	Zn	As	Cd	Pb	Mn
Sediment	5.8	526.3	8.0	88.5	614.0	18225.7	30.0	691.0	49.1	11006.5
Mix Lime-2	9.0	235.4	9.8	79.2	357.4	885.5	404.1	1.8	21.6	40.4
Mix WMP-2	7.4	463.8	6.8	100.7	300.5	2987.7	37.4	513.1	10.8	1684.9

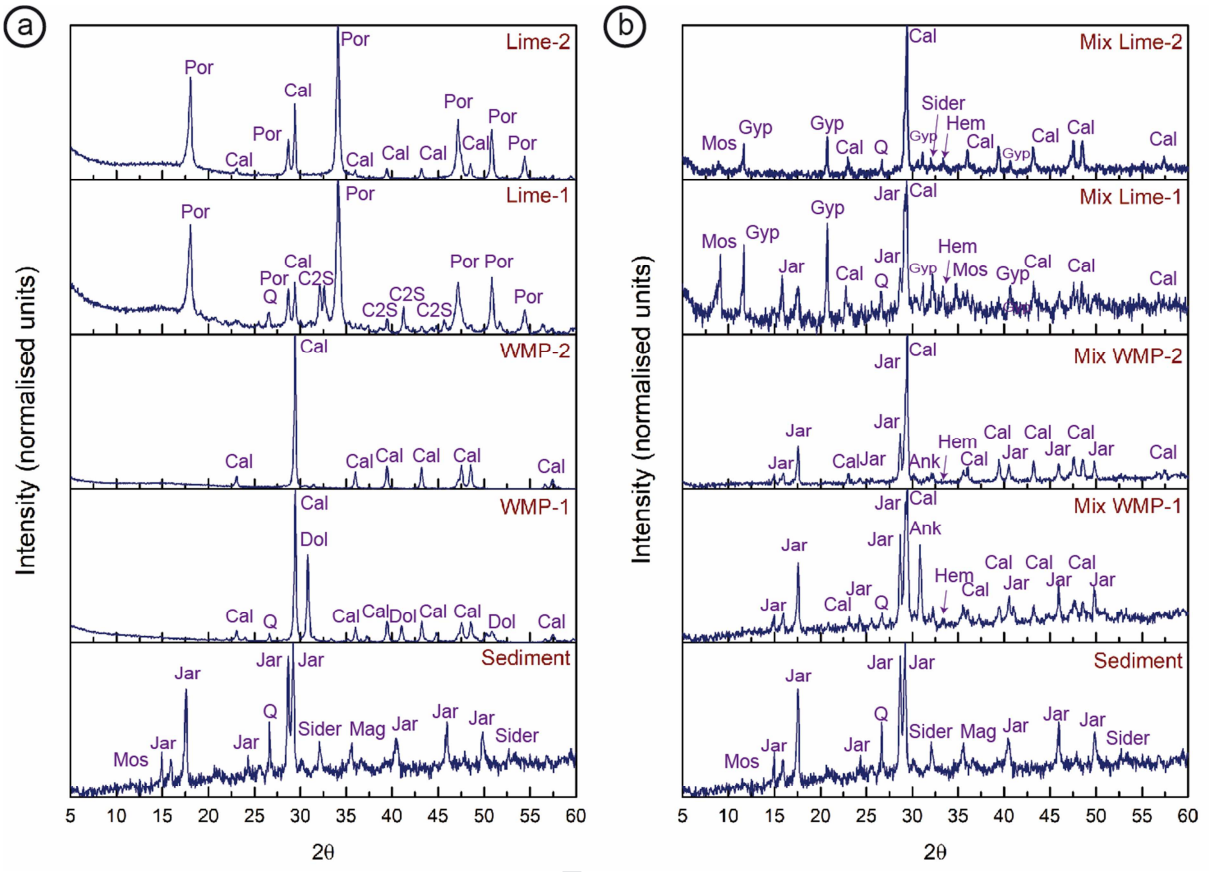

771 *Figure 1. Powder XRD patterns that compare the original sediment to (a) waste marble*
772 *powders (WMP-1 and WMP-2) and lime (Lime-1 and Lime-2) as well as (b) the treated*
773 *sediments. Jar: jarosite; Sider: Siderite; Mag: magnetite; Hem: Hematite; Ank: Ankerite;*
774 *Cal: calcite; Dol: dolomite; Por: Portlandite; Gym: gypsum; Q: quartz; Mos: muscovite;*
775 *C2S: Larnite; Amo: amorphous phase.*

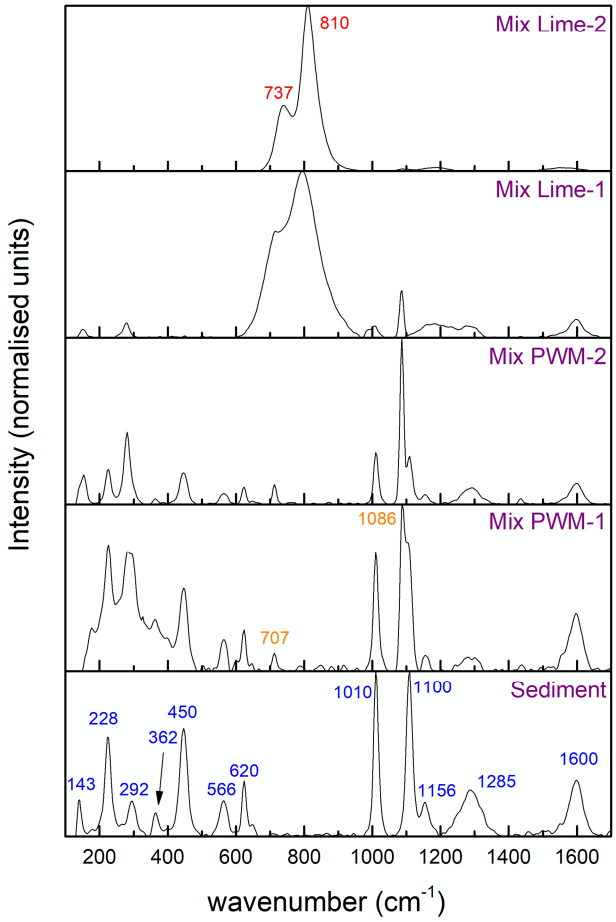

776 *Figure 2. Raman spectra of the original and treated sediments with waste marble powders*
777 *(Mix WMP-1 and Mix WMP-2) and lime (Mix Lime-1 and Mix Lime-2). Bands in blue*
778 *correspond to jarosite, orange to calcite and red to iron oxide-hydroxide phases.*

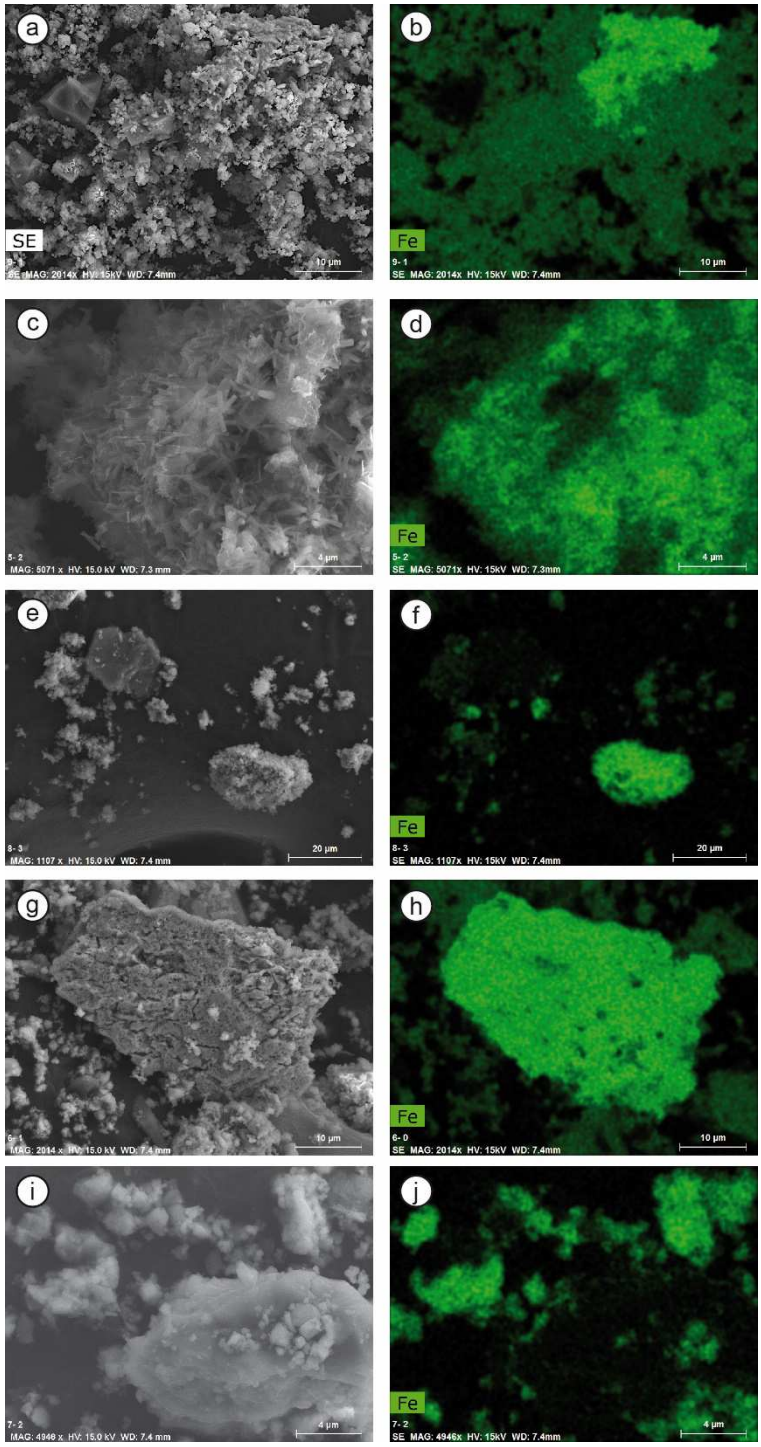

779 *Figure 3. FESEM images and distribution map (mapping) of iron of the original (a-b) and*
780 *treated sediments for Lime-1 (c-d), Lime-2 (c-d), WMP-1 (g-h) and WMP-2 (i-j).*

781

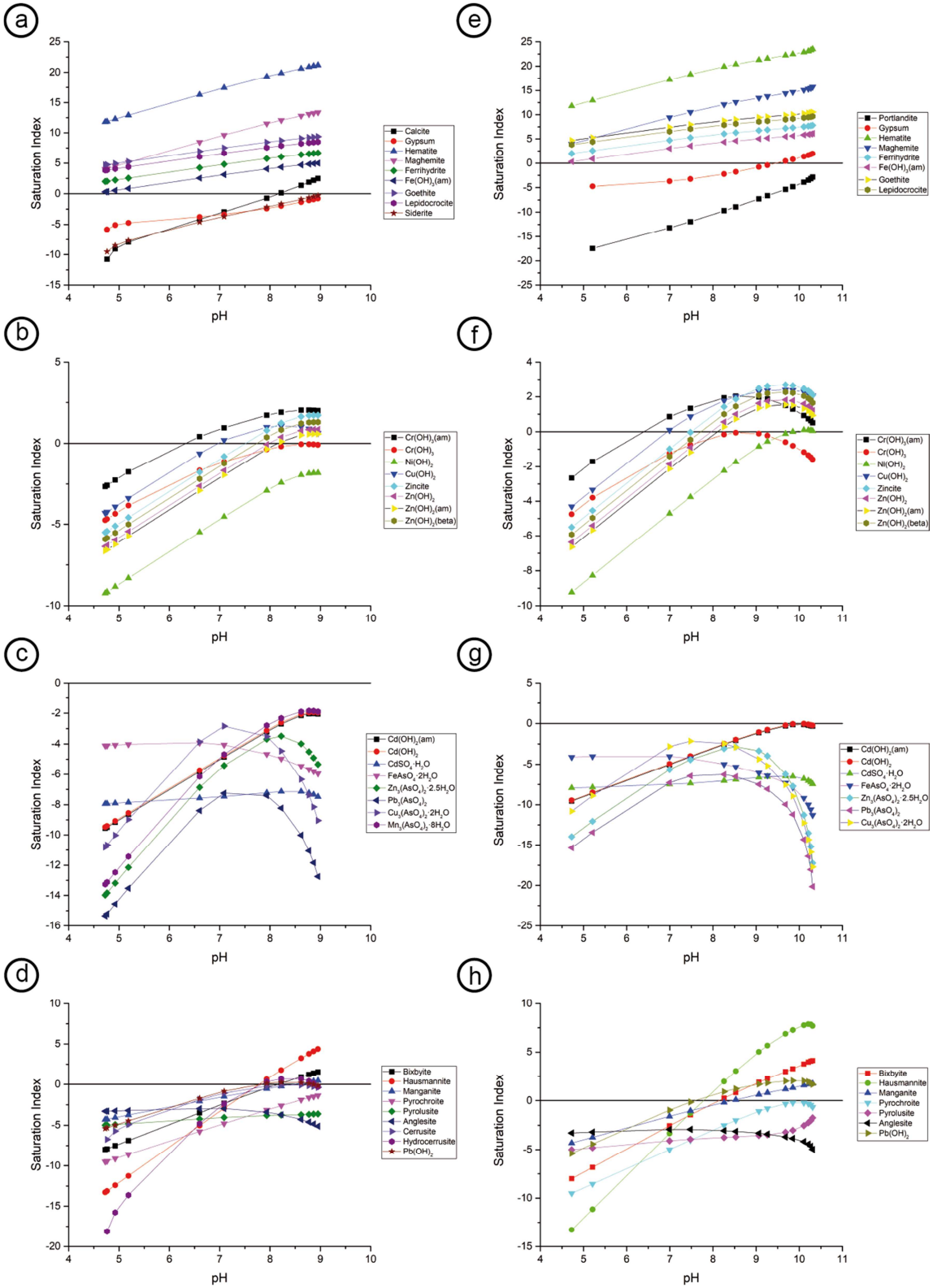

782 Figure 4. Variation of the saturation index of iron, calcium and heavy metals phases with pH
783 by the addition of calcite (a-d) and lime (e-h). Iron and calcium (a,e); chromium, nickel,
784 copper and zinc (b,f); cadmium and arsenic (c,g); manganese and lead phases.

785

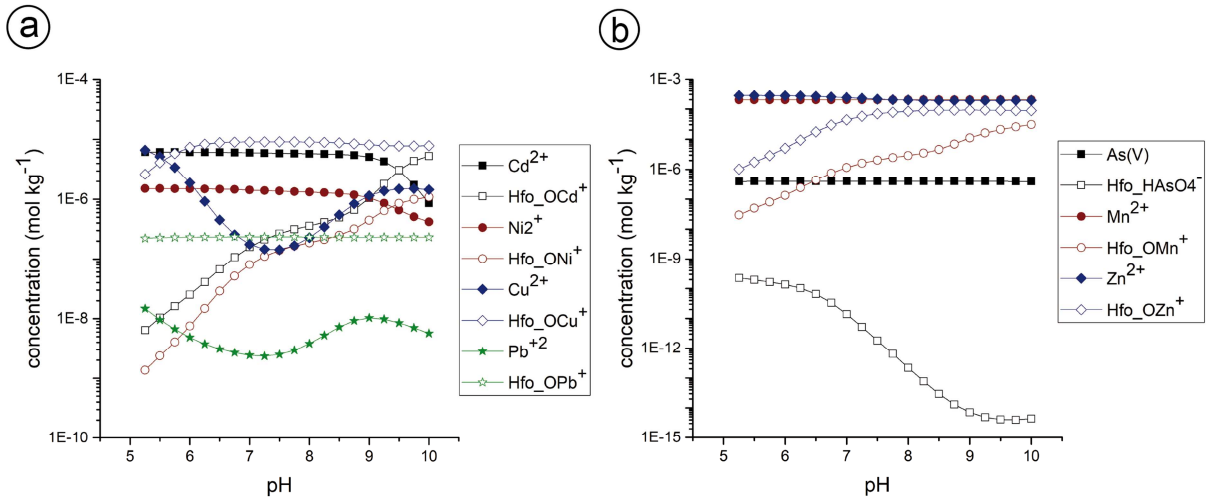

786

787 Figure 5. Variation of concentration of heavy metal in the solution and on the hydrous ferric
788 oxide (Hfo) at different pH values.

Highlights

Jarosite dissolution releases high levels of heavy metals into the environment.

Lime is more effective than calcite-rich waste marble powder in metal immobilisation.

Lime forms hematite, gypsum and calcite and WMP forms hematite and iron carbonates.

The amorphous phases fix heavy metals by sorption and co-precipitation.

Jarosite was eliminated in the lime treatment with major $Ca(OH)_2$ concentration.

Author Contribution Statement

D. Benavente: Conceptualization, Writing - Original Draft, Supervision.

C. Pla: Investigation, Validation, Visualization.

J. Valdes-Abellan: Writing - Review & Editing.

S. Cremades-Alted: Investigation.

Declaration of interests

X The authors declare that they have no known competing financial interests or personal relationships that could have appeared to influence the work reported in this paper.

☐The authors declare the following financial interests/personal relationships which may be considered as potential competing interests: